Neuroradiology (2017) 59:1241–1250
DOI 10.1007/s00234-017-1904-1

FUNCTIONAL NEURORADIOLOGY

# Disease stage-dependent relationship between diffusion tensor imaging and electrophysiology of the visual system in a murine model of multiple sclerosis

**Christopher Nishioka [1,2] · Hsiao-Fang Liang [1,3] · Chen-Fang Chung [1] · Shu-Wei Sun [1,2,3]**

Received: 10 May 2017 / Accepted: 9 August 2017 / Published online: 24 August 2017
© Springer-Verlag GmbH Germany 2017

**Abstract**
*Purpose* Diffusion tensor imaging (DTI) is commonly used to evaluate white matter integrity in multiple sclerosis (MS), but the relationship between DTI measures and functional changes during disease remains ambiguous. Using a mouse model of MS, we tested the hypothesis that DTI measures would correlate to the visual evoked potential (VEPs) dynamically at different disease stages.
*Methods* In vivo DTI, gadolinium-enhanced T1WI (Gd-T1WI) and VEPs were performed in 5 control and 25 mice after 2–12 weeks of experimental autoimmune encephalomyelitis (EAE). DTI indices, including fractional anisotropy (FA), axial and radial diffusivities (AD and RD), and Gd-T1WI enhancement, were measured in the optic nerve and tract (ON and OT), which were compared with measured VEPs.
*Results* Gd-T1WI showed a 3- to 4-fold enhancement over controls beginning after 2 weeks of EAE. Across the time course, we found progressive reductions in FA and increases in RD with increases in VEP latency and reductions in amplitude. Significant correlations between DTI (FA and RD) and VEP evolved; in control/early asymptomatic EAE mice, both FA and RD were highly correlated with VEP latency (but not amplitude), while in late EAE, both DTI indices were highly correlated with VEP amplitude (but not latency).
*Conclusion* DTI measures FA and RD are associated to VEP latency in early stages of EAE but associated to VEP amplitude in later stages, suggesting that the patterns of DTI related to the functional decline may depend on the stage of disease progression.

**Keywords** Diffusion tensor imaging (DTI) · Visual evoked potential (VEP) · Gd-enhanced T1WI (Gd-T1WI) · Experimental autoimmune encephalomyelitis (EAE) · Multiple sclerosis (MS)

**Abbreviations**

| | |
|---|---|
| DTI | Diffusion tensor imaging |
| VEP | Visual evoked potential |
| Gd-T1WI | Gd-enhanced T1-weighted imaging |
| EAE | Experimental autoimmune encephalomyelitis |
| MS | Multiple sclerosis |
| FA | Fractional anisotropy |
| MD | Mean diffusivity |
| AD | Axial diffusivity |
| RD | Radial diffusivity |

## Introduction

Multiple sclerosis (MS) is an inflammatory demyelinating neurodegenerative disease affecting primarily white matter of the central nervous system. Magnetic resonance imaging (MRI) provides critical information to assess MS [1]. Active lesions can be detected using Gd-enhanced T1-weighted imaging (Gd-T1WI), which allows visualization of blood-brain barrier (BBB) permeability [1]. Diffusion tensor imaging (DTI) is sensitive to microstructure changes in white matter tracts. DTI indices including axial diffusivity (AD), radial

✉ Shu-Wei Sun
rsun@llu.edu

[1] Basic Science, School of Medicine, Loma Linda University, 11175 Campus St., Loma Linda, CA 92350, USA

[2] Neuroscience Graduate Program, University of California, Riverside, CA, USA

[3] Pharmaceutical Science, School of Pharmacy, Loma Linda University, Loma Linda, CA, USA

diffusivity (RD), and fractional anisotropy (FA), derived from DTI, can be used to reveal different characteristics of white matter damage including axonal damage and demyelination [2–5]. While these tools are useful for probing the structural characteristics and properties in white matter during MS, it is relatively unclear how they relate to functional outcomes across the spectrum of disease.

The visual system is an ideal model to simulate the structural and functional changes that occur in white matter during MS. The connectivity and electrophysiological properties of the visual system are well characterized [6]. Additionally, the system is frequently affected in MS, especially during bouts of optic neuritis [3–5, 7]. Damage to the visual system can be detected noninvasively by MRI as well as functionally assessed using the visual evoked potential (VEP) [8–10]. However, findings from the relationship between MRI and VEPs have not been consistent. Naismith et al. reported significant correlation between DTI metrics (FA, AD, and RD) and both VEP amplitude and latency [4]. In contrast, two other studies from Trip et al. and Kolbe et al. independently showed significant correlations of DTI only with the VEP amplitude but not with the VEP latency [3, 5]. This discrepancy may be explained by differences in patient populations between these studies; Naismith et al. included patients with optic neuritis incidents within 6 months, while studies by Kolbe et al. and Trip et al. included populations with a mean time since optic neuritis of 4 and 3.1 years, respectively. This difference suggests that DTI measures in white matter may have varying sensitivities to functional nerve properties, depending upon time after initial injury or disease stage.

We hypothesized, based upon results from previous human data, that MRI data would have stronger sensitivity to functional nerve properties at early disease stages vs. late chronic stages. In order to fully appreciate the relationship between structural MRI data and functional changes measured through VEP, we evaluated each during different stages of disease in the commonly used experimental autoimmune encephalomyelitis (EAE) MS model. Using the animal model, the relationship between MRI and VEP was investigated at the acute and chronic stages of EAE. Using this model, we can eliminate much of the individual variability and focus on the manifestation of injury, which will allow a better understanding of how MRI changes correspond to functional decline.

## Materials and methods

### Animal preparation

This study was conducted in accordance with National Institutes of Health guidelines and Statement for the Use of Animals in Ophthalmic and Visual Research and was approved by the Institutional Animal Care and Use Committee in Loma Linda University.

A total of 30 female C57Bl6/WldS mice were used. Five (20 weeks old) were used as controls and 25 (8 weeks old) were EAE induced. For EAE induction, animals were immunized with 60 μg $MOG_{35–55}$ emulsified (1:1) in incomplete Freund's adjuvant (IFA) [11–15]. Pertussis toxin (200 ng; PTX, List Laboratories, Campbell, CA) was injected intraperitoneally on the day of immunization and 3 days later. Five mice were used at each time-point for parallel DTI, Gd-T1WI and VEP at 2-, 4-, 8-, and 12-week post-EAE. Untreated control animals ($N = 5$) were assessed using DTI, Gd-T1, and VEP at 20 weeks of age. An additional five were used to complete a longitudinal DTI study, with scans at baseline (immediately before immunization) and 4-, 8-, and 12-week post-EAE induction. All animals were graded every 2 days for clinical neurological impairment on a scale of 0–5 [11].

### MRI acquisition

Mice were anesthetized by 1.5% isoflurane/oxygen using an isoflurane vaporizer (Vet Equip, Pleasanton, CA). Body temperature was maintained at 37 °C using a warm water heating pad. Scans were collected using a Bruker 11.7T BioSpec small animal MRI instrument. The acquisition protocol used a slice thickness 0.5 mm, FOV of 1.5 cm × 1.5 cm and matrix 128 × 128 (zero filling to 256 × 256), TR 2.5 s, TE 29 ms, $\Delta$ 20 ms, $\delta$ 3 ms, and 21-direction diffusion scheme with $b$ values of 0 and 0.85 ms/μm$^2$ [16]. Using FSL, raw DWIs were corrected for eddy current and motion distortions (http://fsl.fmrib.ox.ac.uk/fsl/). Corrected scans were then imported into 3D Slicer, where eigenvalues ($\lambda_1$, $\lambda_2$, and $\lambda_3$) derived from the diffusion tensor were used to calculate AD, RD, MD, and FA, defined by the following equations

$$\mathrm{AD} = \lambda_1 \tag{1}$$

$$\mathrm{RD} = (\lambda_2 + \lambda_3)/2 \tag{2}$$

$$\mathrm{MD} = (\lambda_1 + \lambda_2 + \lambda_3)/3 \tag{3}$$

$$\mathrm{FA} = \frac{\sqrt{3}\sqrt{(\lambda_1 - MD)^2 + (\lambda_2 - MD)^2 + (\lambda_3 - MD)^2}}{\sqrt{2}\sqrt{(\lambda_1)^2 + (\lambda_2)^2 + (\lambda_3)^2}} \tag{4}$$

DTI measurements were made by manually selecting regions of interest (ROIs). The high anisotropy and low RD of the analyzed regions (optic nerve and tract) provided contrast against neighboring CSF and gray matter to accurately define the regions (Fig. 1).

Blood-brain barrier (BBB) permeability was assessed using gadolinium-enhanced T1-weighted imaging (TR = 0.5 s and

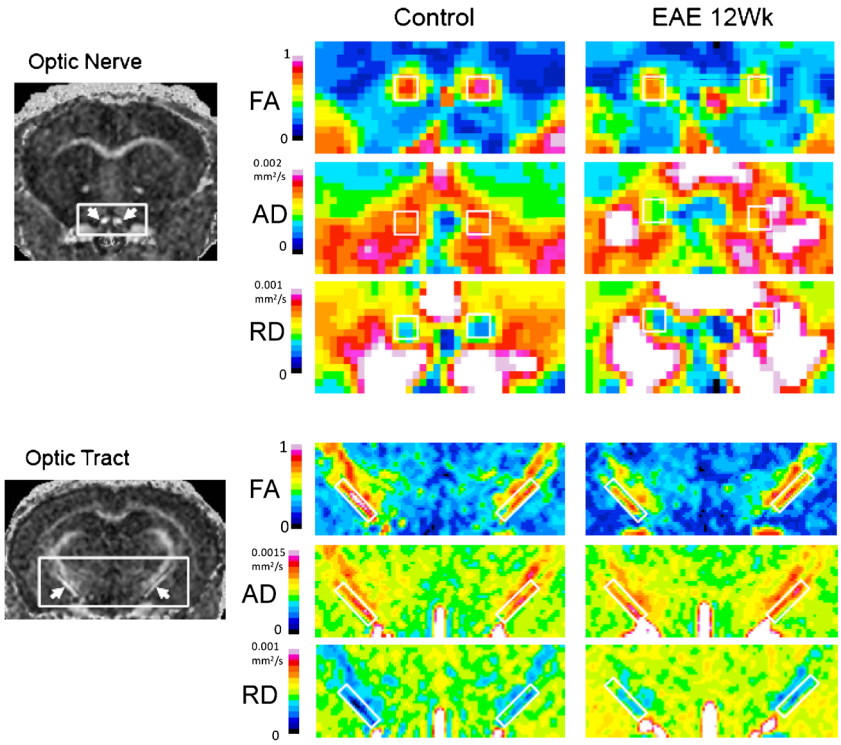


**Fig. 1** DTI maps from the optic nerve and optic tract. FA maps show the location of the ON and OT (left), with individual diffusion index maps shown on the right. Diffusion maps are pseudocolored to show changes in each metric, with ON and OT regions of interests outlined in white. After 12 weeks of EAE, the ON has reductions in FA and increases in RD vs. controls. Alterations in the OT are less obvious, with only small reductions in anisotropy and increases in RD

TE = 14.5 ms). Mice were scanned before and 20 min after a 40-μL gadolinium contrast agent (Omniscan, Amersham Health) injection. Selection of the optic nerve and tract ROI was made using a T2-weighted Rapid Acquisition with Refocused Echoes (RARE) with TR 1 s, echo train 4, and effective TE of 28 ms. Signal intensity in the optic nerve and tract were normalized using background signal from surrounding air and calculated as a percent increase over baseline scans.

### VEP recordings

VEP recordings were performed as previously described [10]. Briefly, animals were anesthetized with a mixture of oxygen and isoflurane (1.5%). Body temperature was maintained at 37 °C throughout the experiment using a water-circulating heating pad. The mouse was mounted into a stereotaxic rig and a midline incision was made through the skin to expose the skull. Two small holes were drilled above the visual cortex (0.5 mm rostral, 2 mm lateral to lambda) and cerebellum (1 mm caudal to lambda). Care was taken to make minimum disturbance to the underlying brain tissue. For VEP recordings, a small loop of silver wire was overlaid on the surface of the visual cortex. Before recording, mice were dark adapted for 10 min. Light stimulation was applied to the eye contralateral to the recording site using an LED light source at frequency of 0.2 Hz with a duration of 5 ms. Field potentials were recorded using a CyberAmp380 amplifier (Molecular Devices, Sunnyvale, CA) and a Digidata1440A interface (Molecular Devices, Sunnyvale, CA), with a sampling rate of 20 kHz and a bandpass filter of 0.1–300 Hz, controlled by Clampex 10.2 (Molecular Devices, Sunnyvale, CA). Averaged data from 100 continuous traces was used to calculate VEP endpoints, including N1 and P1 latency and amplitude. Latency and amplitude of the principal components of the VEP signal (N1 and P1) were measured using Clampfit.

### Statistics

Group data are shown as mean ± standard deviation. A one-way ANOVA was used to compare group means, which was followed by a post-hoc Tukey's test. Statistical comparisons were considered significant at $p < 0.05$. All correlations between DTI data, VEP measures, and Gd-enhancement were evaluated using a Pearson's correlation coefficient. Correlations between average EAE scores and DTI, VEP, and Gd-enhancement measures were performed using Spearman's *r*. Data manipulation and statistical analysis were carried out on Prism GraphPad v6.0.

## Results

### Clinical score

The clinical scores are summarized in Fig. 2. After EAE induction, mice started to develop noticeable behavioral deficits after 2–3 weeks. The earliest symptom was a limp tail

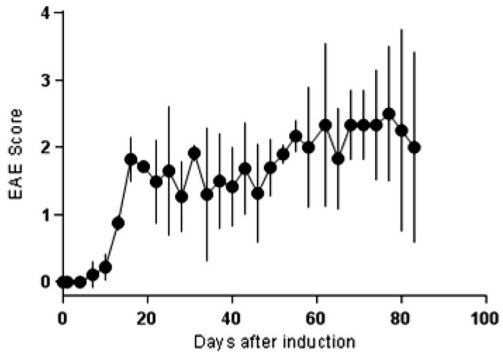


**Fig. 2** Clinical scores of mice affected by EAE. Mice began to show symptoms 2–3 weeks after EAE induction

(score 1), which progressed to hindlimb weakness (score 2) and eventual hindlimb paralysis (unilateral—score 3, bilateral—score 4). Average EAE scores were calculated for each mouse in the 2 weeks preceding time of sacrifice.

## DTI findings

After EAE induction, evidence of damage in the visual pathway was discernible on DTI maps (Fig. 1). A summary of our DTI data in the ON and OT across the time course is shown in Fig. 3. FA trended down while RD trended up. Beginning at 4 weeks, significant DTI changes were observed with a 6.5% reduction of FA in ON ($p = 0.042$), a 22.3% increase of RD in ON ($p = 0.021$), and 17.6% increase of RD in OT ($p = 0.027$). Changes in AD were mixed; only at 8 weeks, a 10% reduction in ON was significant ($p = 0.005$).

## VEP results

Averaged VEP waveforms from each cohort across the time course are shown in Fig. 4. The sharp VEP waveform gradually became less defined over the span of EAE. Despite this feature, the first two major peaks, N1 and P1, were easily identified. The latencies and the amplitude of N1 and P1 were quantified, showing gradual increases in latency and gradual reductions in amplitude with longer durations of disease (Fig. 4). Both measures showed significance relative to the controls beginning at 4 weeks with a 28.1% reduction in amplitude ($p = 0.003$) and a 14.0% increase in latency ($p = 0.045$), which reached a 49.6% reduction in amplitude ($p = 0.0004$) and a 28.2% increase in latency ($p = 0.01$) after 12 weeks.

## Gadolinium-enhancement

Blood-brain barrier integrity was assessed using Gd-T1WI. A significant 3- to 4-fold signal enhancement ($p = 0.017$–$0.002$) was found in the ON at all time-points beginning 2 weeks after EAE induction (Fig. 5), while there was no significant changes in enhancement in the OT.

## VEP and DTI correlation analyses

For comparisons between VEP and DTI data, DTI of each side of the visual pathway (averaged between ON and contralateral OT) was used to compare with acquired VEP signal. The comparisons between VEP and DTI data revealed several

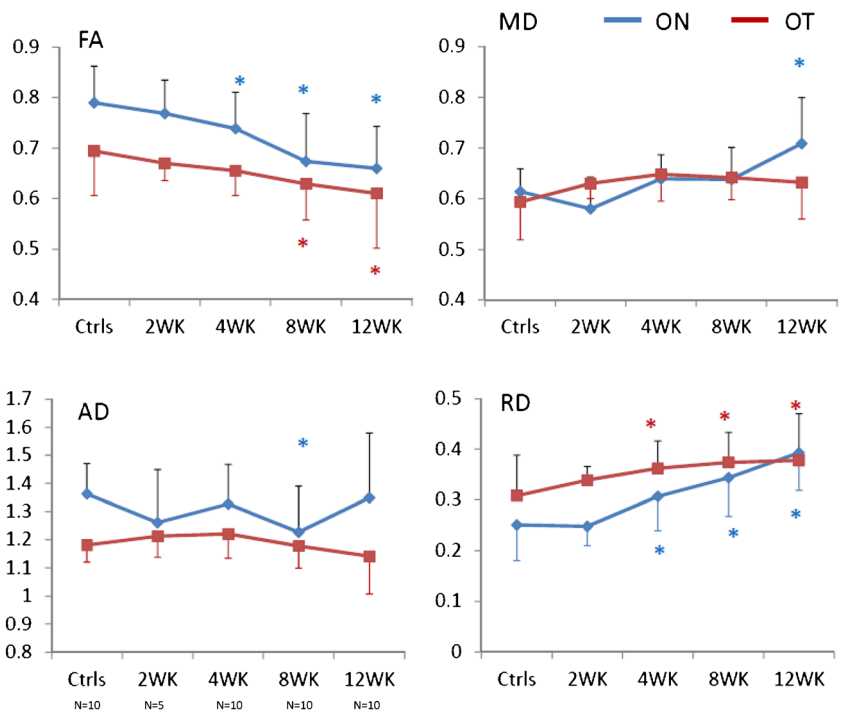


**Fig. 3** DTI measurements from the optic nerve and tract. With increasing durations of EAE, the ON and OT have reductions in FA, increases in RD, and inconsistent changes in AD. "Asterisk" indicates a $p < 0.05$ compared to controls

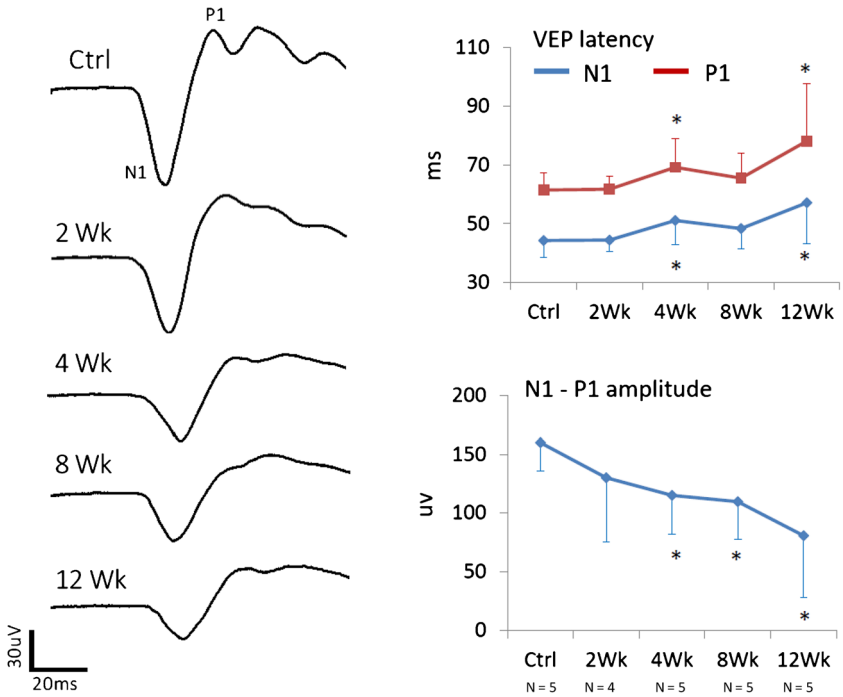


**Fig. 4** Averaged VEP waveforms from each experimental cohort. VEPs are increased in latency and reduced in amplitude with longer durations of EAE. "Asterisk" indicates a $p < 0.05$ compared to controls

significant linear correlations (Table 1; Fig. 6). We found striking differences between control mice and mice with very early EAE (control and 2-week EAE mice) vs. mice at late stages of EAE (8 and 12 week EAE mice). Control and 2-week-EAE mice showed strong relationships between VEP latency and FA ($r = -0.79$, $p = 0.0001$) as well as RD ($r = 0.85$, $p = 0.0003$) (Table 1; Fig. 6). Interestingly, these same mice showed no significant relationship between VEP amplitude and DTI measures. Conversely, mice at late stages of EAE showed strong relationships between reduced VEP amplitude and decreased FA ($r = 0.74$, $p = 0.0002$) and increased RD ($r = -0.73$, $p = 0.0003$) (Table 1; Fig. 6). In these mice, however, VEP latency did not correlate with DTI indices.

### VEP and gadolinium enhancement correlation

As shown in Table 1, across all mice, we observed a significant negative relationship between VEP amplitude and Gd-enhancement ($r = -0.497$, $p = 0.0004$). This relationship was significant both during early (2 weeks) and later stages (8 weeks) of EAE (Fig. 7b). We saw no significant relationship between enhancement and latency ($r = 0.207$, $p = 0.16$).

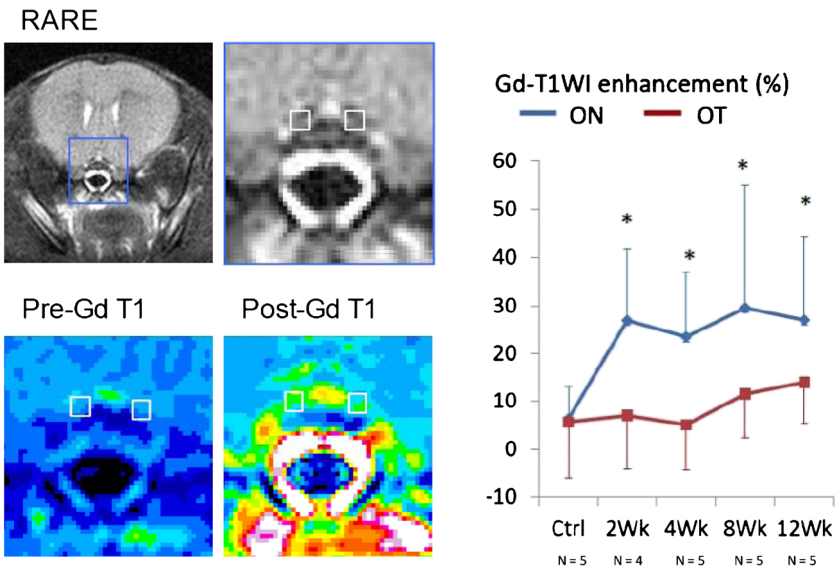


**Fig. 5** Gadolinium enhancement reveals potential BBB leakage in the ON. Top left, RARE image shows coronal slice with optic nerves outlined in white (right). Bottom left, T1 images show signal enhancement after gadolinium. Quantification (right) of enhancement in the ON and OT after Gd-injection shows selective increases above control levels in the ON but not OT. "Asterisk" indicates a $p < 0.05$ compared to controls

**Table 1** Summary of DTI, VEP, and Gd data correlations

| Cohort | | N1 Latency | | N1-P1 Amplitude | | Gd-enhancement | |
|---|---|---|---|---|---|---|---|
| | | Pearson *r* | *p* value | Pearson *r* | *p* value | Pearson *r* | *p* value |
| All mice | FA | *− 0.405* | *0.0039* | *0.555* | *< 0.0001* | − 0.241 | 0.0996 |
| *N* = 24 | RD | *0.488* | *0.0004* | *− 0.518* | *0.0002* | 0.183 | 0.213 |
| | AD | 0.017 | 0.9088 | 0.237 | 0.1054 | − 0.183 | 0.212 |
| | Gd | 0.207 | 0.1627 | *− 0.497* | *0.0004* | x | x |
| Control | FA | *− 0.843* | *0.0022* | − 0.458 | 0.1833 | 0.259 | 0.4702 |
| *N* = 5 | RD | *0.916* | *0.0002* | 0.502 | 0.1392 | − 0.469 | 0.1721 |
| | AD | − 0.115 | 0.7518 | − 0.115 | 0.7518 | − 0.287 | 0.422 |
| | Gd | − 0.355 | 0.3143 | − 0.591 | 0.0722 | x | x |
| 2 weeks | FA | *− 0.719* | *0.0443* | 0.206 | 0.6251 | 0.167 | 0.6935 |
| *N* = 4* | RD | 0.694 | 0.0560 | − 0.207 | 0.6231 | − 0.043 | 0.919 |
| | AD | − 0.029 | 0.9455 | − 0.029 | 0.9455 | 0.489 | 0.218 |
| | Gd | 0.236 | 0.574 | *− 0.809* | *0.015* | x | x |
| 4 weeks | FA | 0.180 | 0.6189 | 0.030 | 0.9341 | − 0.701 | 0.0525 |
| *N* = 5 | RD | − 0.044 | 0.9036 | 0.175 | 0.6281 | 0.581 | 0.1311 |
| | AD | 0.402 | 0.2499 | 0.401 | 0.2499 | − 0.171 | 0.685 |
| | Gd | − 0.389 | 0.3396 | 0.0583 | 0.8909 | x | x |
| 8 weeks | FA | 0.323 | 0.3629 | 0.599 | 0.0673 | − 0.0906 | 0.8035 |
| *N* = 5 | RD | − 0.370 | 0.2921 | − 0.557 | 0.0945 | − 0.0294 | 0.9358 |
| | AD | − 0.046 | 0.8997 | − 0.046 | 0.8997 | − 0.363 | 0.302 |
| | Gd | 0.588 | 0.0741 | *− 0.67* | *0.0339* | x | x |
| 12 weeks | FA | − 0.320 | 0.3381 | *0.782* | *0.0075* | − 0.35 | 0.2648 |
| *N* = 5 | RD | 0.441 | 0.1739 | *− 0.778* | *0.0081* | 0.372 | 0.2333 |
| | AD | − 0.130 | 0.7031 | − 0.130 | 0.7031 | − 0.218 | 0.497 |
| | Gd | 0.332 | 0.3193 | − 0.155 | 0.669 | x | x |

Total numbers of mice from each condition are listed. Each mouse includes two independent data points (e.g., *N* = 5 mice, 10 optic nerves/tracts). Significant correlations at $p < 0.05$ are shown in italics

*The 2-week time-point includes *N* = 4 mice due to early death of one mouse

We also did not observe any significant relationships between Gd-enhancement and any DTI indices.

### Clinical evaluations correlated to VEP, gadolinium enhancement, and DTI measures

Average EAE scores in mice with appreciable disease activity (4-, 8-, and 12-week cohorts) were compared with all DTI, VEP, and Gd data (Table 2). Significant correlations were found between average EAE score and RD ($r = 0.387$, $p = 0.029$) as well as FA at 4 weeks ($r = -0.714$, $p = 0.021$).

## Discussion

In this study, we demonstrate parallel changes of DTI, Gd-T1WI, and VEPs to characterize disease progression though the visual pathway in mice affected by EAE. Our findings are largely in agreement with data from human MS studies [3–5]. In MS, Gd-T1WI is a powerful tool for assessing disease activity [17–19], and our study showed that significant changes in Gd-enhancement was the first indication of disease activity, preceding overt behavioral, functional or diffusional differences. After the onset of EAE, we found continuous reductions in FA and increases in RD within the visual pathway white matter which paralleled gradual decreases in VEP amplitude and increases in VEP latency.

A novel finding from our data is the differentiation of the DTI-VEP relationship in animals at early and late stages of disease. In both control and asymptomatic mice 2 weeks after EAE induction, a significant correlation exists between VEP latency (but not the amplitude) and DTI metrics FA and RD. This is in contrast to data at late disease stages, where significant correlations are between VEP amplitude (instead of the latency) and DTI metrics FA and RD. We interpret our finding to suggest that during basal conditions, FA and RD may be especially sensitive to microstructural differences in myelination, which could explain tight correlation to VEP latency. Our observations may be related to data obtained from human infants, in which VEP latency, instead of amplitude,

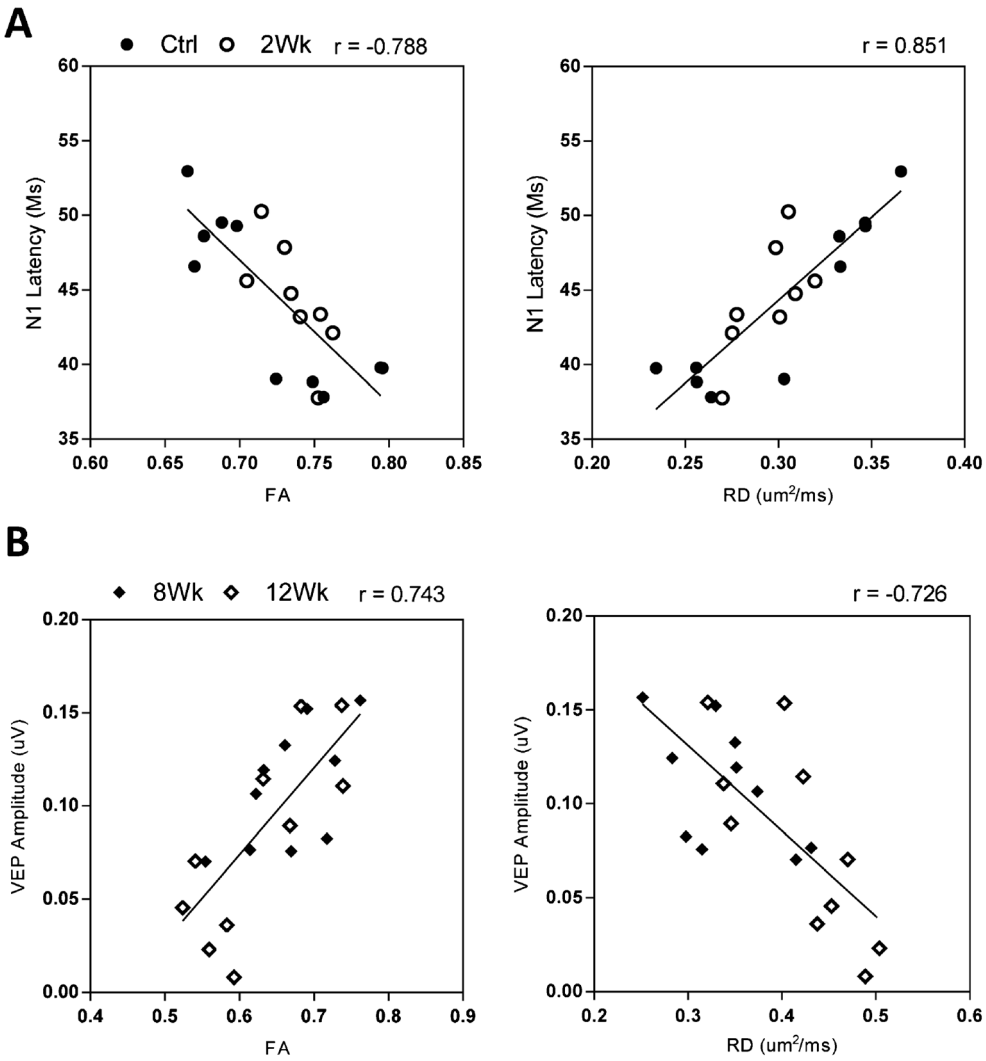


**Fig. 6** Significant relationships between VEP and DTI data. VEP latency and amplitude are correlated with DTI data at different stages of disease severity. **a** VEP latency is closely correlated to FA and RD measures in control and 2-week EAE mice, without any significant linear relationship at later stages of EAE (8 and 12 weeks). **b** In contrast, VEP amplitude shows little relation to DTI measures during early stages of disease but correlates well after 8 and 12 weeks of EAE. Each mouse includes two independent data points (e.g., $N = 5$ mice, 10 optic nerves/tracts). The 2-week time-point includes $N = 4$ mice due to early death of one mouse

shows significant correlation to DTI metrics [20]. VEP latency is highly affected by changes in myelination, both in development [21] and during demyelinating conditions [22]. Additionally, mouse models of demyelination have suggested that FA and RD are indeed very sensitive to small changes in myelination [23, 24]. At the later stages of EAE, cumulative demyelination, inflammation, and axonal damage become prominent [25–27], which affect VEP amplitude and may sensitize DTI measures to differences in axon density. These findings help explain inconsistent literature concerning the relationship between DTI data and VEP signal latency and amplitude [3–5, 7]. Our experiment suggests that the ability of DTI to predict neurological functions may be disease-stage dependent in MS.

Several studies have been conducted using human tissue to examine the connection between DTI data and histology outcomes in MS brain and spinal cord samples [28–31]. These studies may shed light on the pathological factors that influence the DTI signal. Results from this work have demonstrated that DTI parameters, especially that FA and RD are sensitive to demyelination [29–31]. Less clear is the relationship between axonal loss and DTI parameters, which has been associated with AD in MS mouse models [32, 33], but not generally observed in human tissue [30]. FA, RD, and MD have been shown to correlate with axonal counts in white matter [28–30], though work by Schmierer et al. suggests that this correlation may be driven primarily by differences in myelin content [28, 29]. Overall, these data show that DTI appears to be an accurate surrogate measure of demyelination and potentially axonal losses, though the results must be interpreted with several caveats. Importantly, these studies employed different imaging parameters, such as diffusion time and direction encoding schemes. For imaging of tissue specimens, the fixation processes may also affect the DTI signal [34]. Additionally, these studies include extremely varied MS populations, making any distinctions between histological patterns, disease stage and DTI difficult. In light of our mouse data, it may be interesting to reexamine the

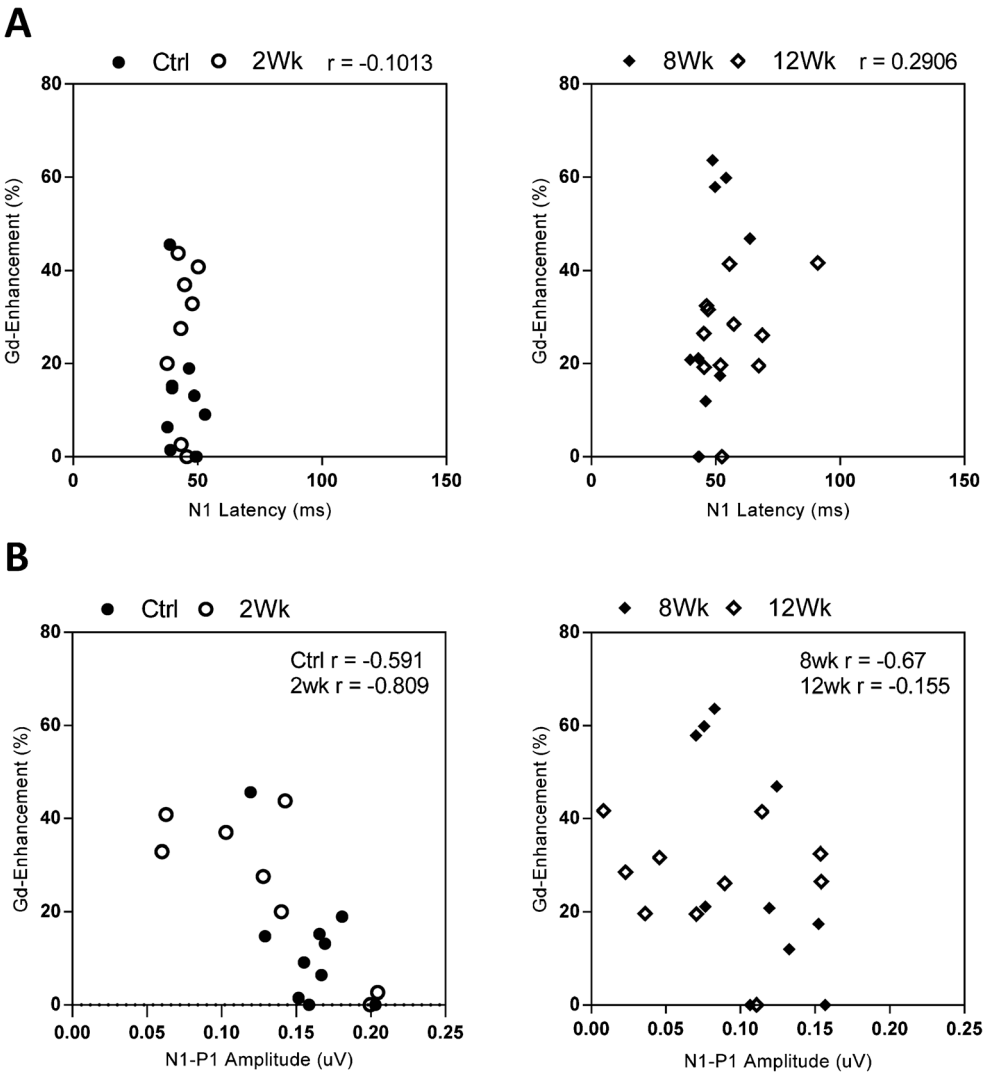


**Fig. 7** Relationships between VEP measurements and ON-Gd-enhancement. **a** Blood-brain barrier permeability within the ON did not correlate with VEP latency in Control/2-week EAE groups or 8-/12-week EAE groups. **b** Gd-enhancement did show significant relation to VEP amplitude at several stages of EAE in 2- and 8-week EAE groups

**Table 2** Correlations between average EAE scores and DTI, VEP, and Gd data

| Cohort | | Spearman *r* | *p* value | Cohort | | Spearman *r* | *p* value |
|---|---|---|---|---|---|---|---|
| 4, 8, 12 weeks | FA | −0.315 | 0.078 | 8 weeks | FA | −0.055 | 0.608 |
| *N* = 15 | RD | *0.387* | *0.029* | *N* = 5 | RD | −0.028 | 0.667 |
| | AD | 0.113 | 0.54 | | AD | −0.413 | 0.114 |
| | Gd | 0.293 | 0.116 | | Gd | 0.29 | 0.416 |
| | N1 Latency | −0.12 | 0.949 | | N1 Latency | −0.028 | 0.667 |
| | N1-P1 Amp | 0.017 | 0.928 | | N1-P1 Amp | −0.275 | 0.246 |
| 4 weeks | FA | *−0.714* | *0.0211* | 12 weeks | FA | 0.086 | 0.795 |
| *N* = 5 | RD | 0.591 | 0.0831 | *N* = 5 | RD | −0.279 | 0.329 |
| | AD | 0.098 | 0.81 | | AD | −0.093 | 0.709 |
| | Gd | 0.683 | 0.083 | | Gd | 0.394 | 0.206 |
| | N1 Latency | −0.443 | 0.183 | | N1 Latency | −0.328 | 0.275 |
| | N1-P1 Amp | 0.197 | 0.602 | | N1-P1 Amp | 0.44 | 0.204 |

Average EAE scores were calculated as an average of the previous 2 weeks' score. The 2-week EAE group was omitted from analysis due to the lack of an appreciable score. Significant correlations at $p < 0.05$ are shown in italics

connection between DTI metrics and histology in newer vs. older lesions.

In addition to indicating damage in the visual pathways, VEPs may correlate broadly with changes in the brain. A study by Lobsien et al. using Tract-Based Spatial Statistics (TBSS) examined white matter across the brain (not including the optic nerve) and compared with VEP signal [35]. They found significant correlation between white matter microstructure alterations and VEP latency in several regions, including regions with no direct role in the visual pathway such as the fornix, as well as structures with a well-defined role for visual pathway, as in the optic radiation. Their work suggests that functional deficits in the visual system may signal more general white matter damage across the brain in MS.

To our knowledge, this study is among the first to define the DTI-VEP relationship using an animal model of MS. Although there is a lack of journal articles, studies with preliminary results have been presented in conference settings [36, 37]. However, none of these presentations have demonstrated the importance of disease stage in determining the relationship between functional and microstructure data.

In conclusion, we compared measurements from DTI, Gd-T1WI, and VEPs to quantify structural and functional deficits in mice affected by EAE. Gd-T1WI detects early alterations in BBB integrity, while DTI changes (especially RD and FA) correlate with increasing VEP latency and reduced amplitude. The ability of DTI to predict VEP latency and amplitude depends upon the stage of disease. The data suggests that information about disease stage may advance the use of DTI data to predict functional changes in the nervous system during MS.

**Acknowledgements** We thank Dr. Wei-Xing Shi, Pharmaceutical Science, Loma Linda University, for an insightful discussion.

**Compliance with ethical standards**

**Funding information** This work was funded in part by NIH R01 NS062830 and the National Space Biomedical Research Institute (RE03701) through the National Aeronautics and Space Administration NCC 9–58.

**Conflict of interest** The authors declare that they have no conflict of interest.

**Ethical approval** All applicable international, national, and/or institutional guidelines for the care and use of animals were followed. All procedures performed in studies involving animals were in accordance with the ethical standards of the institution or practice at which the studies were conducted.

**Informed consent** Statement of informed consent was not applicable since the manuscript does not contain any patient data.

## References

1. Polman CH, Reingold SC, Banwell B, Clanet M, Cohen JA, Filippi M, Fujihara K, Havrdova E, Hutchinson M, Kappos L, Lublin FD, Montalban X, O'Connor P, Sandberg-Wollheim M, Thompson AJ, Waubant E, Weinshenker B, Wolinsky JS (2011) Diagnostic criteria for multiple sclerosis: 2010 revisions to the McDonald criteria. Ann Neurol 69(2):292–302. doi:10.1002/ana.22366
2. Nishioka C, Poh C, Sun SW (2015) Diffusion tensor imaging reveals visual pathway damage in patients with mild cognitive impairment and Alzheimer's disease. J Alzheimers Dis 45(1):97–107. doi:10.3233/JAD-141239
3. Trip SA, Wheeler-Kingshott C, Jones SJ, Li WY, Barker GJ, Thompson AJ, Plant GT, Miller DH (2006) Optic nerve diffusion tensor imaging in optic neuritis. NeuroImage 30(2):498–505. doi:10.1016/j.neuroimage.2005.09.024
4. Naismith RT, Xu J, Tutlam NT, Trinkaus K, Cross AH, Song SK (2010) Radial diffusivity in remote optic neuritis discriminates visual outcomes. Neurology 74(21):1702–1710. doi:10.1212/WNL.0b013e3181e0434d
5. Kolbe S, Chapman C, Nguyen T, Bajraszewski C, Johnston L, Kean M, Mitchell P, Paine M, Butzkueven H, Kilpatrick T, Egan G (2009) Optic nerve diffusion changes and atrophy jointly predict visual dysfunction after optic neuritis. NeuroImage 45(3):679–686. doi:10.1016/j.neuroimage.2008.12.047
6. Chalupa LM, Williams RW (2008) Eye, retina, and visual system of the mouse. MIT Press, Cambridge
7. Davies MB, Williams R, Haq N, Pelosi L, Hawkins CP (1998) MRI of optic nerve and postchiasmal visual pathways and visual evoked potentials in secondary progressive multiple sclerosis. Neuroradiology 40(12):765–770
8. Sun SW, Liang HF, Schmidt RE, Cross AH, Song SK (2007) Selective vulnerability of cerebral white matter in a murine model of multiple sclerosis detected using diffusion tensor imaging. Neurobiol Dis 28(1):30–38. doi:10.1016/j.nbd.2007.06.011
9. Sun SW, Liang HF, Cross AH, Song SK (2008) Evolving Wallerian degeneration after transient retinal ischemia in mice characterized by diffusion tensor imaging. NeuroImage 40(1):1–10. doi:10.1016/j.neuroimage.2007.11.049
10. Sun SW, Liang HF, Mei J, Xu D, Shi WX (2014) In vivo diffusion tensor imaging of amyloid-beta-induced white matter damage in mice. J Alzheimers Dis 38(1):93–101. doi:10.3233/JAD-130236
11. Cross AH, Misko TP, Lin RF, Hickey WF, Trotter JL, Tilton RG (1994) Aminoguanidine, an inhibitor of inducible nitric oxide synthase, ameliorates experimental autoimmune encephalomyelitis in SJL mice. J Clin Invest 93(6):2684–2690. doi:10.1172/JCI117282
12. Cross AH, Girard TJ, Giacoletto KS, Evans RJ, Keeling RM, Lin RF, Trotter JL, Karr RW (1995) Long-term inhibition of murine experimental autoimmune encephalomyelitis using CTLA-4-fc supports a key role for CD28 costimulation. J Clin Invest 95(6):2783–2789
13. Cross AH, San M, Keeling RM, Karr RW (1999) CTLA-4-Fc treatment of ongoing EAE improves recovery, but has no effect upon relapse rate. Implications for the mechanisms involved in disease perpetuation. J Neuroimmunol 96(2):144–147
14. Kerlero de Rosbo N, Mendel I, Ben-Nun A (1995) Chronic relapsing experimental autoimmune encephalomyelitis with a delayed onset and an atypical clinical course, induced in PL/J mice by myelin oligodendrocyte glycoprotein (MOG)-derived peptide: preliminary analysis of MOG T cell epitopes. Eur J Immunol 25(4):985–993
15. Lyons JA, San M, Happ MP, Cross AH (1999) B cells are critical to induction of experimental allergic encephalomyelitis by protein but not by a short encephalitogenic peptide. Eur J Immunol 29(11):3432–3439

16. Hasan KM, Narayana PA (2003) Computation of the fractional anisotropy and mean diffusivity maps without tensor decoding and diagonalization: theoretical analysis and validation. Magn Reson Med 50(3):589–598. doi:10.1002/mrm.10552
17. Barkhof F, Filippi M, Miller DH, Scheltens P, Campi A, Polman CH, Comi G, Ader HJ, Losseff N, Valk J (1997) Comparison of MRI criteria at first presentation to predict conversion to clinically definite multiple sclerosis. Brain 120(Pt 11):2059–2069
18. Miller DH, Barkhof F, Nauta JJ (1993) Gadolinium enhancement increases the sensitivity of MRI in detecting disease activity in multiple sclerosis. Brain 116(Pt 5):1077–1094
19. Sormani MP, Bruzzi P (2013) MRI lesions as a surrogate for relapses in multiple sclerosis: a meta-analysis of randomised trials. Lancet Neurol 12(7):669–676. doi:10.1016/S1474-4422(13)70103-0
20. Dubois J, Dehaene-Lambertz G, Soares C, Cointepas Y, Le Bihan D, Hertz-Pannier L (2008) Microstructural correlates of infant functional development: example of the visual pathways. J Neurosci 28(8):1943–1948. doi:10.1523/JNEUROSCI.5145-07.2008
21. Tsuneishi S, Casaer P (1997) Stepwise decrease in VEP latencies and the process of myelination in the human visual pathway. Brain and Development 19(8):547–551
22. You Y, Klistorner A, Thie J, Graham SL (2011) Latency delay of visual evoked potential is a real measurement of demyelination in a rat model of optic neuritis. Invest Ophthalmol Vis Sci 52(9):6911–6918. doi:10.1167/iovs.11-7434
23. Sun SW, Liang HF, Trinkaus K, Cross AH, Armstrong RC, Song SK (2006) Noninvasive detection of cuprizone induced axonal damage and demyelination in the mouse corpus callosum. Magn Reson Med 55(2):302–308. doi:10.1002/mrm.20774
24. Song SK, Yoshino J, Le TQ, Lin SJ, Sun SW, Cross AH, Armstrong RC (2005) Demyelination increases radial diffusivity in corpus callosum of mouse brain. NeuroImage 26(1):132–140. doi:10.1016/j.neuroimage.2005.01.028
25. Craner MJ, Lo AC, Black JA, Waxman SG (2003) Abnormal sodium channel distribution in optic nerve axons in a model of inflammatory demyelination. Brain 126(Pt 7):1552–1561. doi:10.1093/brain/awg153
26. Bettelli E, Pagany M, Weiner HL, Linington C, Sobel RA, Kuchroo VK (2003) Myelin oligodendrocyte glycoprotein-specific T cell receptor transgenic mice develop spontaneous autoimmune optic neuritis. J Exp Med 197(9):1073–1081. doi:10.1084/jem.20021603
27. Xu J, Sun SW, Naismith RT, Snyder AZ, Cross AH, Song SK (2008) Assessing optic nerve pathology with diffusion MRI: from mouse to human. NMR Biomed 21(9):928–940. doi:10.1002/nbm.1307
28. Schmierer K, Wheeler-Kingshott CA, Boulby PA, Scaravilli F, Altmann DR, Barker GJ, Tofts PS, Miller DH (2007) Diffusion tensor imaging of post mortem multiple sclerosis brain. NeuroImage 35(2):467–477. doi:10.1016/j.neuroimage.2006.12.010
29. Schmierer K, Wheeler-Kingshott CA, Tozer DJ, Boulby PA, Parkes HG, Yousry TA, Scaravilli F, Barker GJ, Tofts PS, Miller DH (2008) Quantitative magnetic resonance of postmortem multiple sclerosis brain before and after fixation. Magn Reson Med 59(2):268–277. doi:10.1002/mrm.21487
30. Klawiter EC, Schmidt RE, Trinkaus K, Liang HF, Budde MD, Naismith RT, Song SK, Cross AH, Benzinger TL (2011) Radial diffusivity predicts demyelination in ex vivo multiple sclerosis spinal cords. NeuroImage 55(4):1454–1460. doi:10.1016/j.neuroimage.2011.01.007
31. Zollinger LV, Kim TH, Hill K, Jeong EK, Rose JW (2011) Using diffusion tensor imaging and immunofluorescent assay to evaluate the pathology of multiple sclerosis. J Magn Reson Imaging 33(3):557–564. doi:10.1002/jmri.22502
32. Budde MD, Xie M, Cross AH, Song SK (2009) Axial diffusivity is the primary correlate of axonal injury in the experimental autoimmune encephalomyelitis spinal cord: a quantitative pixelwise analysis. J Neurosci 29(9):2805–2813. doi:10.1523/JNEUROSCI.4605-08.2009
33. Budde MD, Kim JH, Liang HF, Russell JH, Cross AH, Song SK (2008) Axonal injury detected by in vivo diffusion tensor imaging correlates with neurological disability in a mouse model of multiple sclerosis. NMR Biomed 21(6):589–597. doi:10.1002/nbm.1229
34. Sun SW, Liang HF, Xie M, Oyoyo U, Lee A (2009) Fixation, not death, reduces sensitivity of DTI in detecting optic nerve damage. NeuroImage 44(3):611–619. doi:10.1016/j.neuroimage.2008.10.032
35. Lobsien D, Ettrich B, Sotiriou K, Classen J, Then Bergh F, Hoffmann KT (2014) Whole-brain diffusion tensor imaging in correlation to visual-evoked potentials in multiple sclerosis: a tract-based spatial statistics analysis. AJNR Am J Neuroradiol 35(11):2076–2081. doi:10.3174/ajnr.A4034
36. Santangelo R, Castoldi V, Camaleonti L, Cursi M, Dina G, Comi G, Quattrini A, Chaabane L, Leocani L (2015) Visual evoked potentials and MRI in monitoring optic nerve involvement in a relapsing remitting model of EAE. Clin Neurophysiol 126(1):e9. doi:10.1016/j.clinph.2014.10.054
37. Xu D, Liang HF, Shi W, Sun SW (2011) Correlation between DTI and visual evoked potential in mice with optic neuritis. 19th Annual Meeting of ISMRM-ESMRMB, Montreal, p 2309